



## Large-scale structural alteration of brain in epileptic children with *SCN1A* mutation



Yun-Jeong Lee<sup>a,1,2</sup>, Mi-Sun Yum<sup>a,1</sup>, Min-Jee Kim<sup>a</sup>, Woo-Hyun Shim<sup>b</sup>, Hee Mang Yoon<sup>b</sup>,  
Il Han Yoo<sup>c</sup>, Jiwon Lee<sup>d</sup>, Byung Chan Lim<sup>e</sup>, Ki Joong Kim<sup>e,\*</sup>, Tae-Sung Ko<sup>a,\*\*</sup>

<sup>a</sup> Department of Pediatrics, Asan Medical Center Children's Hospital, University of Ulsan College of Medicine, Seoul, Republic of Korea

<sup>b</sup> Department of Radiology, Asan Medical Center, University of Ulsan College of Medicine, Seoul, Republic of Korea

<sup>c</sup> Department of Pediatrics, St. Vincent's Hospital, The Catholic University of Korea, Suwon, Republic of Korea

<sup>d</sup> Department of Pediatrics, Samsung Medical Center, Sungkyunkwan University School of Medicine, Seoul, Republic of Korea

<sup>e</sup> Department of Pediatrics, Seoul National University Children's Hospital, Seoul, Republic of Korea

### ARTICLE INFO

#### Keywords:

*SCN1A*  
Epilepsy  
Magnetic resonance imaging  
Brain volume  
Surface area  
Children

### ABSTRACT

**Objective:** Mutations in *SCN1A* gene encoding the alpha 1 subunit of the voltage gated sodium channel are associated with several epilepsy syndromes including genetic epilepsy with febrile seizures plus (GEFS+) and severe myoclonic epilepsy of infancy (SMEI). However, in most patients with *SCN1A* mutation, brain imaging has reported normal or non-specific findings including cerebral or cerebellar atrophy. The aim of this study was to investigate differences in brain morphometry in epileptic children with *SCN1A* mutation compared to healthy control subjects.

**Methods:** We obtained cortical morphology (thickness, and surface area) and brain volume (global, subcortical, and regional) measurements using FreeSurfer (version 5.3.0, <https://surfer.nmr.mgh.harvard.edu>) and compared measurements of children with epilepsy and *SCN1A* gene mutation ( $n = 21$ ) with those of age and gender matched healthy controls ( $n = 42$ ).

**Results:** Compared to the healthy control group, children with epilepsy and *SCN1A* gene mutation exhibited smaller total brain, total gray matter and white matter, cerebellar white matter, and subcortical volumes, as well as mean surface area and mean cortical thickness. A regional analysis revealed significantly reduced gray matter volume in the patient group in the bilateral inferior parietal, left lateral orbitofrontal, left precentral, right postcentral, right isthmus cingulate, right middle temporal area with smaller surface area and white matter volume in some of these areas. However, the regional cortical thickness was not significantly different in two groups.

**Significance:** This study showed large-scale developmental brain changes in patients with epilepsy and *SCN1A* gene mutation, which may be associated with the core symptoms of the patients. Further longitudinal MRI studies with larger cohorts are required to confirm the effect of *SCN1A* gene mutation on structural brain development.

### 1. Introduction

The *SCN1A* gene (MIM#182389), which encodes the alpha 1 subunit of the voltage-gated sodium channel, is the most clinically identified gene associated with epilepsy. The spectrum of epilepsy related to

*SCN1A* mutation spans from milder phenotypes, such as genetic epilepsy with febrile seizures plus (GEFS+), to severe myoclonic epilepsy of infancy (SMEI), also known as Dravet syndrome (Gambardella and Marini, 2009). GEFS+ is characterized by recurrent febrile seizure events beyond 5–6 years of age, even up to the teenage years, and can

**Abbreviation:** CSF, cerebrospinal fluid; GEFS+, genetic epilepsy with febrile seizures plus; GM, gray matter; MRI, magnetic resonance imaging; SMEI, severe myoclonic epilepsy of infancy; TIV, total intracranial volume; WM, white matter

\* Correspondence to: K. J. Kim, Pediatric Clinical Neuroscience Center, Seoul National University Children's Hospital, 101 Daehak-ro, Jongno-gu, Seoul 110-744, Republic of Korea.

\*\* Correspondence to: T.-S. Ko, Department of Pediatrics, Asan Medical Center Children's Hospital, University of Ulsan College of Medicine, 88 Olympic-ro 43-gil, Songpa-gu, Seoul 05505, Republic of Korea.

E-mail addresses: [pednr@plaza.snu.ac.kr](mailto:pednr@plaza.snu.ac.kr) (K.J. Kim), [tsko@amc.seoul.kr](mailto:tsko@amc.seoul.kr) (T.-S. Ko).

<sup>1</sup> These authors contributed equally to the manuscript.

<sup>2</sup> Present address: Department of Pediatrics, Kyungpook National University Children's Hospital, Daegu, Republic of Korea.

<http://dx.doi.org/10.1016/j.nicl.2017.06.002>

Received 14 February 2017; Received in revised form 1 May 2017; Accepted 1 June 2017

Available online 06 June 2017

2213-1582/ © 2017 The Authors. Published by Elsevier Inc. This is an open access article under the CC BY-NC-ND license (<http://creativecommons.org/licenses/by-nc-nd/4.0/>).

develop a number of afebrile heterogeneous seizure types with remission in adolescence (Scheffer and Berkovic, 1997; Camfield and Camfield, 2015). Dravet syndrome is a deleterious form of childhood epilepsy characterized by recurrent febrile and afebrile seizures in the first year, followed by multiple seizure types resistant to various anti-epileptic drugs, as well as cognitive, behavioral, and motor impairment (Dravet, 2011). Mutation of *SCN1A* has been detected in 60–80% of patients with Dravet syndrome and, in contrast, only 10% of patients with GEFS+ (Brunklau et al., 2012; Marini et al., 2011; Scheffer et al., 2009).

Although it remains to be elucidated which modifying factors are responsible for the different phenotypes of *SCN1A* mutation-related epilepsy, (Brunklau et al., 2012; Mistry et al., 2014; Zuberi et al., 2011) previously published reports are largely in agreement on the role of decreased excitability of GABAergic inhibitory interneurons leading to an imbalance between excitation and inhibition in a selective area of the brain as a pathogenesis of *SCN1A* mutation-related epilepsy (Yu et al., 2006; Ogiwara et al., 2007; Cheah et al., 2012). Although this altered synaptic activity might not be the only mechanism that shapes connectivity patterns in brain, it will change the pattern of refinement of activity dependent neural circuitry during brain development (Tessier and Broadie, 2009; Flores and Mendez, 2014). We hypothesized that there would be large-scale structural changes in the brains of patients with *SCN1A* mutation as the result of altered synaptic activities and brain development. However, few data are available on the neuroimaging and neuropathology of epileptic patients with *SCN1A* mutation. Previous studies were unable to find specific or consistent neuroimaging findings related to *SCN1A* mutation (Brunklau et al., 2012; Guerrini et al., 2011; Striano et al., 2007; Moehring et al., 2013). Furthermore, the majority of patients with *SCN1A* mutation exhibited no gross structural brain abnormalities with the exception of a few minor findings, including cerebral or cerebellar atrophy, cortical dysplasia, or hippocampal sclerosis (Brunklau et al., 2012; Guerrini et al., 2011; Striano et al., 2007). Therefore, quantitative neuroimaging approaches such as brain volumetry and cortical morphometry may be useful in assessing the structural changes which could not otherwise be seen by conventional brain magnetic resonance imaging (MRI), and in understanding the pathogenesis of *SCN1A* mutation. Herein, we compared brain volume and cortical morphology in patients with *SCN1A* mutation-positive epilepsy and healthy control group as well as analyzed differences in the developmental patterns of their brains.

## 2. Methods

### 2.1. Subjects

Epileptic patients with *SCN1A* mutation were recruited from the pediatric neurology clinics of three medical centers in Korea: Asan Medical Center, Samsung Medical Center, and Seoul National University Children's Hospital. We included patients who satisfied the following inclusion criteria: (i) epilepsy diagnosed by a pediatric neurologist; (ii) genetically confirmed *SCN1A* mutation; (iii) normal brain MRI. All patients underwent brain MRI for the diagnostic evaluation of epilepsy, and all images were interpreted by one pediatric neuroradiologist (HM Yoon), who confirmed that the images were free of any brain abnormalities. We collected patients' clinical information, including age, sex, seizure onset, seizure phenotype, occurrence of status epilepticus during follow-up, resistance to multiple antiepileptic drug, cognitive and behavioral outcome, and *SCN1A* mutation type.

For each patient, two healthy control subjects matched in age and gender and without alleged neurologic deficits were recruited. All MRIs of the controls were reviewed and interpreted as normal by the same pediatric neuroradiologist (HM Yoon). Our study protocol was approved by the Institutional Review Board of all participating institutions (Asan Medical Center, Samsung Medical Center, Seoul National University Children's Hospital).

### 2.2. MRI acquisition

MRI scans were obtained on a Philips Achieva 3.0T scanner (Philips Healthcare, Eindhoven, The Netherlands) ( $n = 53$ ) and Siemens MAGNETOM Verio 3.0T scanner (Siemens AG, Erlangen, Germany) ( $n = 10$ ). Three-dimensional whole brain T1 sequence imaging was acquired with the following image parameters: echo time (TE) = 4.6 ms, repetition time (TR) = 9.8 ms, flip angle (FA) = 8.08, field of view (FOV) = 224 × 224 mm, matrix = 256 × 256, slice thickness = 1 mm, sagittal images of the entire brain with in-plane resolution 1.0 mm × 1.0 mm or TE = 5.1 ms, TR = 25 ms, FA = 30, FOV = 220 × 220 mm, matrix = 512 × 512, slice thickness = 1 mm, sagittal images of the entire brain with in-plane resolution 1.0 mm × 1.0 mm on a Philips 3.0 T Achieva scanner. On the MAGNETOM Verio scanner, images were obtained with TE = 1.9 ms, TR = 1500 ms, FA = 9.0, FOV = 220 × 220 mm, matrix = 256 × 256, slice thickness = 1 mm, sagittal images of the entire brain with in-plane resolution 1.0 mm × 1.0 mm. Before data processing, all raw T1 sequencing images were visually inspected for common MR T1 weighted imaging artifacts, which can undermine segmentation accuracy, by an experienced researcher (WH Shim) and neuroradiologist (HM Yoon).

### 2.3. Image analyses

All measurements, including cortical thickness, surface area, and volume were obtained from T1 MRI scans using FreeSurfer (version 5.3.0, <https://surfer.nmr.mgh.harvard.edu>), a fully automated surface-based analysis. The technical details of the procedures have been previously described (Dale et al., 1999; Fischl et al., 1999; Fischl and Dale, 2000; Fischl et al., 2004). Briefly, the processing pipeline included correcting of intensity variation, removal of non-brain tissue, segmentation of the gray matter/white matter (GM/WM) tissue, tessellation of the cortical GM/WM boundary, inflation of the folded surfaces, and automatic correction of topological defects to detect GM/WM and GM/cerebrospinal fluid (CSF) boundaries. Cortical thickness was quantified as the closest distance from the GM/WM boundary to the GM/CSF boundary at each vertex. Subcortical volumes were calculated with FreeSurfer's automated procedure for volumetric measures. Each voxel in the normalized brain volumes were assigned to one of 40 labels, including cerebellum and brain stem (Fischl et al., 2004). Cortical volume, cortical thickness, and surface area were estimated for 34 regions per hemisphere according to the Desikan FreeSurfer atlas (Desikan et al., 2006). To improve accuracy of imaging analysis, key intermediate processing outputs (skull stripping, segmentation, parcellation) of FreeSurfer were visually inspected and, if needed, brain masks and inaccurate definitions of white matters were manually corrected by a trained researcher (WH Shim) as described in FreeSurfer website.<sup>3</sup>

### 2.4. Statistical analyses

We compared age and gender distributions between groups using *t*-tests and chi-square tests. FreeSurfer's built-in general linear model tool, QDEC, was performed to compare regional cortical thickness between groups, controlling for age and gender. Cortical thickness data were smoothed with a 10 mm full width at half maximum (FWHM) Gaussian kernel. To correct for multiple comparisons, the false discovery rate (FDR) was implemented using a cluster-wise correction method with an initial cluster-forming threshold set at  $p < 0.01$ . Only clusters with a corrected value of  $p < 0.05$  were considered to be significant. Analysis of covariance (ANCOVA) was performed using SPSS version 18.0 (SPSS, Chicago, IL) to compare group differences in the mean cortical thickness, mean surface area, and volume (global volume and regional volume) with age and gender as covariates. In surface area and volumetric analysis, total intracranial volume (TIV)

<sup>3</sup> [https://surfer.nmr.mgh.harvard.edu/fswiki/FsTutorial/WhiteMatterEdits\\_freeview](https://surfer.nmr.mgh.harvard.edu/fswiki/FsTutorial/WhiteMatterEdits_freeview).

**Table 1**  
Demographic data of patient and control group.

|  | Patient group   | Control group   | p-Value |
|--|-----------------|-----------------|---------|
| Number of subjects, n                        | 21              | 42              |         |
| Age (months), mean $\pm$ SD                  | 57.8 $\pm$ 30.1 | 59.1 $\pm$ 29.8 | 0.878   |
| Sex (male)                                   | 7 (33.3%)       | 14 (33.3%)      | 1.0     |
| Age at seizure onset (months), mean $\pm$ SD | 8.1 $\pm$ 7.8   | –               | –       |
| Status epilepticus, n (%)                    | 11 (52.4%)      | –               | –       |
| Psychomotor status, n (%)                    |                 | –               | –       |
| Normal intelligence                          | 3 (14.3%)       |                 |         |
| Mild mental retardation                      | 8 (38.1%)       |                 |         |
| Moderate mental retardation                  | 8 (38.1%)       |                 |         |
| Severe mental retardation                    | 2 (9.5%)        |                 |         |
| Ataxia, n (%)                                | 4 (19%)         | –               | –       |

was included as a covariate to control the total brain size. Bonferroni correction for multiple comparisons was applied, and a  $p < 0.0015$  was considered to be significant for both the cortical volume and surface area analysis for 34 regions ( $p < 0.05/34$ ) as well as the analysis of 35 subcortical structural volumes ( $p < 0.05/35$ ). We also assessed age-related group differences using QDEC (cortical thickness) and ANCOVA in SPSS (volume, surface area) after adjusting age and gender. The measurements in whole-brain analysis and age-related group differences were considered as significant with a value of  $p < 0.05$ .

### 3. Results

#### 3.1. Demographical and clinical characteristics

A total of 21 patients and 42 healthy control subjects were recruited. All demographic and clinical characteristic data from the patient and healthy control groups are shown in Table 1 and Inline Supplementary Table S1.

Inline Supplementary Table S1 can be found online at <http://dx.doi.org/10.1016/j.nicl.2017.06.002>.

#### 3.2. Whole-brain analysis

There was no significant difference in the total intracranial volume (TIV) between the two groups ( $p = 0.09$ ). After controlling for age, sex, and TIV, the total brain, total GM, total cortical GM, subcortical GM, total cortical WM, and cerebellar WM, total cerebellar volumes of the patient group were significantly smaller than those of the healthy control group, while the cerebellar GM was not different (Table 2). The mean cortical surface area and cortical thickness were significantly reduced in the patient group, with a much larger discrepancy in surface area (difference between means:  $-5.5%$ ,  $p < 0.001$ ) than in cortical

thickness (difference between means:  $-2.4%$ ,  $p = 0.045$ ).

#### 3.3. Effect of age on volume, cortical thickness and surface area

We compared the age effect on cortical thickness, global volume and surface area between the two groups. In comparison with the control group, there was no observed statistically significant difference in terms of age effect on total brain ( $p = 0.056$ ), total GM ( $p = 0.076$ ), total cortical GM ( $p = 0.077$ ), total cortical WM ( $p = 0.097$ ), cerebellar WM ( $p = 0.276$ ) and cerebellar GM volume ( $p = 0.192$ ), mean cortical thickness ( $p = 0.344$ ) and mean surface area ( $p = 0.134$ ). (Fig. 1).

The scatter plots show the age effect on total brain volume (A), total cortical gray matter volume (B), total gray matter volume (C), and total cortical white matter volume (D). CM, control male group; CF, control female group; PM, patient male group; PF, patient female group.

#### 3.4. Subcortical volume analysis

Subcortical volume analysis was performed to compare the volumes of the subcortical structures (thalamus, caudate, putamen, pallidum, hippocampus, accumbens area, CSF, and corpus callosum), cerebellum, and brainstem between the patient and control groups. After correction for multiple comparisons, the patient group showed significantly reduced volumes in bilateral putamen, caudate, accumbens area compared to the control group (corrected  $p$ -value  $< 0.05$ ) (Table 3).

#### 3.5. Regional analysis of volume, surface area, cortical thickness

After correction for multiple comparisons, a regional surface area analysis of 34 parcellated regions per hemisphere found that patients had significantly decreased surface areas in the left lateral orbitofrontal and right middle temporal area (Table 4). Also, the patient group

**Table 2**  
Whole-brain analysis.

| Measurement              | Patient group        | Control group          | p-Value <sup>a</sup> | Difference between means (%) |
|--------------------------|----------------------|------------------------|----------------------|------------------------------|
| Total brain volume       | 1,010,403 $\pm$ 7425 | 1,061,252 $\pm$ 10,586 | <b>&lt; 0.001</b>    | - 4.8                        |
| Total GM volume          | 659,426 $\pm$ 7990   | 695,315 $\pm$ 5604     | <b>&lt; 0.001</b>    | - 5.2                        |
| Total cortical GM volume | 507,927 $\pm$ 6866   | 543,168 $\pm$ 4816     | <b>&lt; 0.001</b>    | - 6.5                        |
| Subcortical GM volume    | 52,331 $\pm$ 856     | 55,539 $\pm$ 601       | <b>0.004</b>         | - 5.8                        |
| Total cortical WM volume | 330,133 $\pm$ 49,997 | 342,700 $\pm$ 3505     | <b>0.046</b>         | - 3.7                        |
| Cerebellar WM volume     | 21,226 $\pm$ 669     | 23,800 $\pm$ 470       | <b>0.003</b>         | - 10.8                       |
| Cerebellar GM volume     | 99,844 $\pm$ 2054    | 97,836 $\pm$ 1440      | 0.43                 | + 2.0                        |
| Total cerebellum volume  | 121,070 $\pm$ 2289   | 121,636 $\pm$ 1605     | <b>0.040</b>         | - 0.5                        |
| Mean surface area        | 151,530 $\pm$ 1923   | 160,271 $\pm$ 1349     | <b>&lt; 0.001</b>    | - 5.5                        |
| Mean cortical thickness  | 2.83 $\pm$ 0.03      | 2.90 $\pm$ 0.02        | <b>0.045</b>         | - 2.4                        |

Data are presented as mean  $\pm$  standard deviation.

Bold font indicates statistical significance ( $p < 0.05$ ).

Volume is expressed in mm<sup>3</sup>, surface area in mm<sup>2</sup>, and thickness in mm.

GM, gray matter; WM, white matter.

<sup>a</sup>  $p$ -Values from general linear model after controlling age, gender and total intracranial volume (for the cortical thickness, only age and gender are included as covariate).

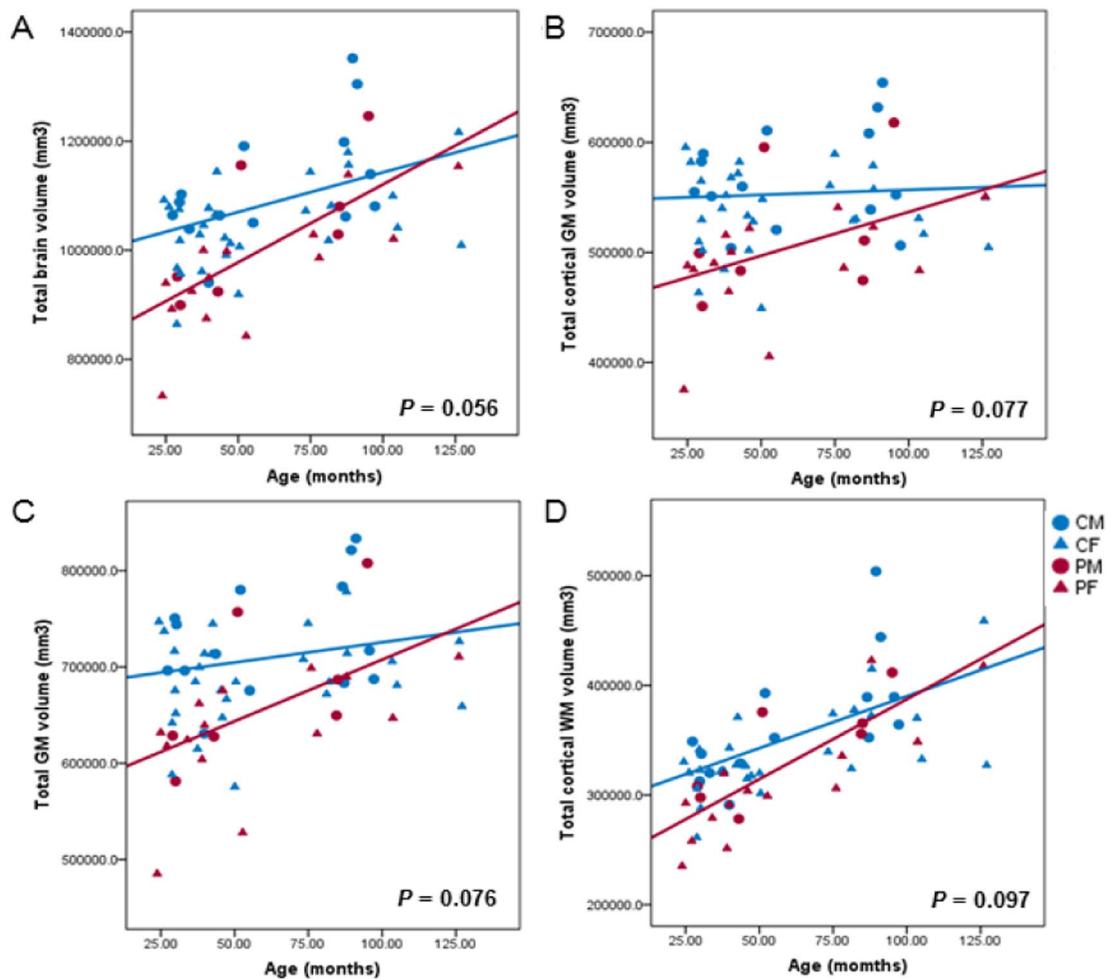


Fig. 1. Linear correlations between age and global volume in the patient and control groups.

showed a significantly smaller GM volume in the bilateral inferior parietal, left lateral orbitofrontal, left precentral, right postcentral, right isthmus cingulate, right middle temporal areas (Table 4). In the regional WM volume analysis, the patient group showed a significantly smaller WM volume in the left lateral orbitofrontal area. There was no area where patients group showed statistically significant difference in regional cortical thickness analysis. Regional morphometric findings are described in more detail in the Inline Supplementary Table S2.

Table 3  
Group comparison of subcortical volume analysis.

| Subcortical volume | Patient group | Control group | p-Value <sup>a,*</sup> | Difference between means (%) |
|--------------------|---------------|---------------|------------------------|------------------------------|
| Putamen            |               |               |                        |                              |
| L                  | 5213 ± 167.9  | 5994 ± 117.8  | < 0.001                | -13.0                        |
| R                  | 5248 ± 164.8  | 6002 ± 115.6  | < 0.001                | -12.6                        |
| Caudate            |               |               |                        |                              |
| L                  | 3274 ± 88.0   | 3663 ± 61.7   | < 0.001                | -10.6                        |
| R                  | 3276 ± 90.3   | 3688 ± 63.3   | < 0.001                | -11.2                        |
| Accumbens area     |               |               |                        |                              |
| L                  | 557 ± 33.6    | 703 ± 23.6    | < 0.001                | -20.8                        |
| R                  | 579 ± 34.4    | 736 ± 24.1    | < 0.001                | -21.3                        |

Data are presented as mean ± standard deviation.

Volume expressed in mm<sup>3</sup>.

L, left; R, right.

<sup>a</sup> Age, gender, and total intracranial volume are included as covariates in comparisons between the patient and control groups.

\* Only effects with significant values after correction for multiple comparison.

Inline Supplementary Table S2 can be found online at <http://dx.doi.org/10.1016/j.nicl.2017.06.002>.

#### 4. Discussion

This study aimed to investigate morphometric brain abnormalities in patients with *SCN1A* mutation and related epilepsy. In the whole-brain analysis, we found significantly smaller total brain volume, total cortical GM volume, subcortical GM volume, total cortical WM volume and cerebellar WM volume in the patient group compared to the control group. These volume changes are consistent with previous studies, suggesting non-specific neuroimaging findings, such as atrophic change on cerebral and cerebellar area (Brunklau et al., 2012; Guerrini et al., 2011; Striano et al., 2007) and brain morphometry analysis in patients with Dravet syndrome (Perez et al., 2014). Although the potential mechanism responsible for the volume change is uncertain, functional changes in GABAergic inhibitory interneurons, which are important in normal brain development, can alter the neural network formation (Flores and Mendez, 2014). One report also supports this hypothesis in that it has identified progressively reduced dendritic arborization and excessive spines in dentate gyrus granule cell of the mouse model (*Scn1a<sup>E1099X/+</sup>*) mimicking human Dravet syndrome (Tsai et al., 2015). This same study supports that this microstructural alteration likely results in neural network instability and has an impact on epileptogenesis and higher-order cognitive processing.

In our study, we identified brain developmental patterns in epileptic children with *SCN1A* mutation, which has not previously been shown by routine visual analysis. While patient group exhibited similar trajectories of global brain development of the normal controls, the total

**Table 4**  
Group comparison of surface area, gray matter and white matter volume in 34 parcellated regions.

| Parcellated region         | Surface area <sup>a</sup> |                | GM volume <sup>a</sup> |                | WM volume <sup>a</sup> |       |
|----------------------------|---------------------------|----------------|------------------------|----------------|------------------------|-------|
|                            | Left                      | Right          | Left                   | Right          | Left                   | Right |
| <b>Frontal</b>             |                           |                |                        |                |                        |       |
| Superior frontal           | 0.058                     | 0.027          | 0.029                  | 0.003          | 0.269                  | 0.019 |
| Rostral middle frontal     | 0.043                     | 0.190          | 0.061                  | 0.028          | 0.126                  | 0.455 |
| Caudalmiddle frontal       | 0.287                     | 0.302          | 0.216                  | 0.122          | 0.933                  | 0.224 |
| Pars opercularis           | 0.111                     | 0.396          | 0.116                  | 0.189          | 0.047                  | 0.476 |
| Pars triangularis          | 0.006                     | 0.020          | 0.005                  | 0.009          | 0.009                  | 0.141 |
| Pars orbitalis             | 0.002                     | 0.034          | 0.029                  | 0.004          | 0.029                  | 0.150 |
| Lateral orbitofrontal      | < <b>0.001</b>            | 0.082          | < <b>0.001</b>         | 0.464          | < <b>0.001</b>         | 0.033 |
| Medial orbitofrontal       | 0.189                     | 0.052          | 0.294                  | 0.106          | 0.959                  | 0.089 |
| Precentral                 | 0.014                     | 0.728          | <b>0.001</b>           | 0.023          | 0.611                  | 0.343 |
| Paracentral                | 0.007                     | 0.677          | 0.002                  | 0.244          | 0.243                  | 0.443 |
| Frontal pole               | 0.203                     | 0.097          | 0.294                  | 0.121          | 0.597                  | 0.061 |
| Rostral anterior cingulate | 0.074                     | 0.076          | 0.030                  | 0.280          | 0.946                  | 0.494 |
| Caudal anterior cingulate  | 0.174                     | 0.163          | 0.184                  | 0.038          | 0.236                  | 0.451 |
| <b>Parietal</b>            |                           |                |                        |                |                        |       |
| Superior parietal          | 0.562                     | 0.583          | 0.049                  | 0.058          | 0.548                  | 0.410 |
| Inferior parietal          | 0.002                     | 0.002          | < <b>0.001</b>         | < <b>0.001</b> | 0.002                  | 0.043 |
| Supramarginal              | 0.713                     | 0.025          | 0.281                  | 0.006          | 0.488                  | 0.272 |
| Postcentral                | 0.548                     | 0.006          | 0.008                  | < <b>0.001</b> | 0.998                  | 0.059 |
| Precuneus                  | 0.095                     | 0.003          | 0.016                  | 0.002          | 0.098                  | 0.008 |
| Posterior cingulate        | 0.002                     | 0.233          | 0.010                  | 0.248          | 0.035                  | 0.486 |
| Isthmus cingulate          | 0.007                     | 0.011          | 0.040                  | < <b>0.001</b> | 0.038                  | 0.801 |
| <b>Temporal</b>            |                           |                |                        |                |                        |       |
| Superior temporal          | 0.067                     | 0.011          | 0.168                  | 0.020          | 0.700                  | 0.461 |
| Middle temporal            | 0.032                     | < <b>0.001</b> | 0.232                  | < <b>0.001</b> | 0.736                  | 0.035 |
| Inferior temporal          | 0.002                     | 0.123          | 0.017                  | 0.851          | 0.016                  | 0.071 |
| Banks of the STS           | 0.240                     | 0.014          | 0.099                  | 0.015          | 0.267                  | 0.040 |
| Fusiform                   | 0.003                     | 0.191          | 0.041                  | 0.476          | 0.005                  | 0.062 |
| Transverse temporal        | 0.958                     | 0.464          | 0.128                  | 0.089          | 0.584                  | 0.154 |
| Entorhinal                 | 0.320                     | 0.844          | 0.574                  | 0.811          | 0.585                  | 0.649 |
| Temporal pole              | 0.039                     | 0.508          | 0.928                  | 0.173          | 0.623                  | 0.814 |
| Parahippocampal            | 0.155                     | 0.506          | 0.003                  | 0.036          | 0.066                  | 0.504 |
| <b>Occipital</b>           |                           |                |                        |                |                        |       |
| Lateral occipital          | 0.220                     | 0.180          | 0.042                  | 0.071          | 0.878                  | 0.974 |
| Lingual                    | 0.234                     | 0.547          | 0.376                  | 0.432          | 0.302                  | 0.813 |
| Cuneus                     | 0.017                     | 0.256          | 0.014                  | 0.008          | 0.142                  | 0.543 |
| Pericalcarine              | 0.193                     | 0.492          | 0.259                  | 0.042          | 0.474                  | 0.462 |
| Insular cortex             | 0.081                     | 0.630          | 0.215                  | 0.391          | 0.194                  | 0.817 |
| Unsegmented WM             |                           |                |                        |                | 0.038                  | 0.075 |

L, left; R, right; GM, gray matter; WM, white matter.

Bold font indicates statistical significance ( $p < 0.05$ ) after correction for multiple comparisons.

<sup>a</sup> Age, gender, and total intracranial volume were included as covariates in comparisons between the patient and control groups.

brain volume, GM and WM volume showed the largest discrepancy between the patients and controls during early childhood (Fig. 1). There is robust growth in human brain volume, mainly in the gray matter, through the first 2 years of life, with rapid elaboration of dendrites, spines, and synapses (Tau and Peterson, 2010). Synaptic overgrowth in early infancy is essential to ensure the complete wiring of the nervous system (Tessier and Broadie, 2009). Smaller GM volume during early childhood of patients with *SCN1A* mutation may be related to insufficient synaptogenesis and myelination in first 2 years of age, as well as an abnormal cortical pruning process through childhood (Tau and Peterson, 2010).

In our study, we also identified a smaller subcortical volume in the bilateral areas of putamen, caudate, accumbens area in the patients group compared to control group. The basal ganglia neural circuit connected with the cortex and the thalamus plays a key role in the modulation of motor control as well as cognitive and executive function and behavior (Bhatia and Marsden, 1994). The significant subcortical volume changes observed in this study could explain the epileptic seizures, motor impairments and cognitive declines of Dravet syndrome (Dravet, 2011).

In the regional analysis, the patient group exhibited a smaller GM volume in the bilateral inferior parietal, left lateral orbitofrontal, left precentral, right postcentral, right isthmus cingulate, right middle

temporal area with the reduced surface area and WM volume in some of these areas. The inferior parietal, isthmus cingulate, and the middle temporal gyrus comprise the default mode network that influences task performance and the integration of cognitive and emotional processing (Raichle and Mintun, 2006). These structural changes may be related to the widespread alteration of the neuronal network related to epilepsy in patients with *SCN1A* mutation. Previous report also showed activation in areas of the default mode network in patients with Dravet syndrome (Moehring et al., 2013). The lateral orbitofrontal cortex is involved in guiding stimulus based learning and decision making (Walton et al., 2010) and the middle temporal gyrus is involved in a number of cognitive processes, including semantic memory processing, language processes, as well as visual perception and multimodal sensory integration (Davey et al., 2016; Mesulam, 1998). The pre- and post-central areas interact to generate somatosensory and motor function (Nii et al., 1996). The higher incidence of learning difficulties, language delays, motor impairment and behavior disorders in patient with *SCN1A* mutation-related epilepsy (Dravet, 2011; Wolff et al., 2006) can be explained by the reduced size of these areas, which in turn may cause the malfunction of these structures. Conversely, previous brain morphometric analysis in patients with Dravet syndrome revealed no difference in local GM volume (Perez et al., 2014). This discrepancy could be explained differences in the tools used for analysis and/or

characteristics of the enrolled patients, such as the inclusion of younger patient groups irrespective of disease severity. As we noted, the younger patients showed a bigger difference in volume in this study (Fig. 1). However, present study could not clarify exact neuro-anatomical pattern correlated with phenotype since this study included too young patients (mean age at last follow up:  $7.7 \pm 2.9$  years) to define the clinical diagnosis such as Dravet syndrome or GEFS+. Further study with larger patient group will be required to find the stratified results according to the phenotype.

Cortical volume is composed of two independent components, surface area and cortical thickness, which have different ontogenic processes from one another, providing independent information on brain development (Vijayakumar et al., 2016). While cortical thickness depends on the numbers of cells in their intrinsic radial column, surface area is associated with the number of radial columns which can be affected by the inputs from subcortical structures (Rakic, 1988). Also, the volume is more highly correlated with area because volume is a quadratic function of surface distance and only a linear function of thickness (Winkler et al., 2010). In our study, patient group exhibited a much larger discrepancy in mean surface area than mean cortical thickness. Also, most of the regions with reduced GM volume were consistent with the region with smaller surface area in the patient group, while the cortex was not significantly thinner in the patient group than the control group according to the regional cortical thickness analysis. This result is in agreement with previous study suggesting that cortical thickness and surface area were found to be genetically independent (Winkler et al., 2010). The genetic influence of the *SCN1A* mutation may affect separately on cortical thickness and surface area during ontogenic processes.

Additionally, cerebellar WM volume was significantly smaller in patients with *SCN1A* mutations. The cerebellum is involved in motor coordination, balance, and posture, as well as in cognitive functions, such as memory, language, visuospatial skills, and attention (Tedesco et al., 2011; Fine et al., 2002). An experimental mouse model of Dravet syndrome revealed that the impairment of the sodium current and action potential firing in the GABAergic Purkinje neurons of the cerebellum may be responsible for motor coordination (Kalume et al., 2007) and that Purkinje neurons play an important role in cerebellar development and maturation (Fleming and Chiang, 2015). Thus, the core symptoms of Dravet syndrome, including ataxia, poor motor coordination, and autistic behavior, can be explained by these changes to the cerebellum linked to *SCN1A* mutation (Dravet, 2011; Battaglia et al., 2013).

This study has some limitations due to its small sample size and study design in that it is a cross-sectional study and may reflect cohort differences rather than true developmental trajectories. Furthermore, this study only examined linear age effects and interactions exclusively in patients 2–12 years of age, despite the fact that key cortical measures, such as cortical thickness, have been shown to have non-linear developing trajectory through their life (Shaw et al., 2008). Technically, the subjects have been scanned on two different scanners with different parameters, which may influence the GM segmentation. However, all data used in our study were carefully visually inspected by a trained researcher, which may result in more reliable estimates (Iskan et al., 2015). Another limitation is the heterogeneity in patient characteristics in terms of frequency of seizures, developmental status, and genetic subtypes, which may be possible confounding factors. In the future, longitudinal studies with larger sample sizes and wider age ranges should be conducted to detect more accurate developmental trajectories after stratification by patient characteristics.

## 5. Conclusions

Using surface-based morphometric analysis, we found large-scale structural brain alterations associated with *SCN1A* mutation and related epilepsy, which may be linked to the core symptoms of *SCN1A*

mutation-positive epilepsy. Children with *SCN1A* mutation-positive epilepsy showed smaller cortical and subcortical GM and surface area and exhibited changes in developmental trajectory compared to healthy control patients. Future longitudinal and *in vivo* functional studies of *SCN1A* mutation are needed to confirm the effect of *SCN1A* gene mutation on structural brain development.

## Funding

This work was supported by an NRF-2016R1C1B2010078 and a grant (2016-703) from the Asan Institute for Life Sciences, Seoul, Korea.

## Disclosure of conflicts of interest

None of the authors has any conflict of interest to disclose.

## Acknowledgements

The authors would like to thank Sun-Ok Kim (Asan Medical Center) for conducting the statistical analyses and Joo Young Oh (Asan Medical Center) for completing the brain structural analyses.

## References

- Battaglia, D., Chieffo, D., Siracusano, R., Waure, C., Brogna, C., Ranalli, D., et al., 2013. Cognitive decline in Dravet syndrome: is there a cerebellar role? *Epilepsy Res.* 106 (1–2), 211–221.
- Bhatia, K.P., Marsden, C.D., 1994. The behavioural and motor consequences of focal lesions of the basal ganglia in man. *Brain* 117 (Pt 4), 859–876.
- Brunklaus, A., Ellis, R., Reavey, E., Forbes, G.H., Zuberi, S.M., 2012. Prognostic, clinical and demographic features in *SCN1A* mutation-positive Dravet syndrome. *Brain* 135 (Pt 8), 2329–2336.
- Camfield, P., Camfield, C., 2015. Febrile seizures and genetic epilepsy with febrile seizures plus (GEFS+). *Epileptic Disorders* 17 (2), 124–133 *International Epilepsy Journal With Videotape*.
- Cheah, C.S., Yu, F.H., Westenbroek, R.E., Kalume, F.K., Oakley, J.C., Potter, G.B., et al., 2012. Specific deletion of Nav1.1 sodium channels in inhibitory interneurons causes seizures and premature death in a mouse model of Dravet syndrome. *Proc. Natl. Acad. Sci. U. S. A.* 109 (36), 14646–14651.
- Dale, A.M., Fischl, B., Sereno, M.I., 1999. Cortical surface-based analysis. I. Segmentation and surface reconstruction. *NeuroImage* 9 (2), 179–194.
- Davey, J., Thompson, H.E., Hallam, G., Karapanagiotidis, T., Murphy, C., De Caso, I., et al., 2016. Exploring the role of the posterior middle temporal gyrus in semantic cognition: integration of anterior temporal lobe with executive processes. *NeuroImage* 137, 165–177.
- Desikan, R.S., Ségonne, F., Fischl, B., Quinn, B.T., Dickerson, B.C., Blacker, D., et al., 2006. An automated labeling system for subdividing the human cerebral cortex on MRI scans into gyral based regions of interest. *NeuroImage* 31 (3), 968–980.
- Dravet, C., 2011. The core Dravet syndrome phenotype. *Epilepsia* 52 (Suppl. 2), 3–9.
- Fine, E.J., Ionita, C.C., Lohr, L., 2002. The history of the development of the cerebellar examination. *Semin. Neurol.* 22 (4), 375–384.
- Fischl, B., Dale, A.M., 2000. Measuring the thickness of the human cerebral cortex from magnetic resonance images. *Proc. Natl. Acad. Sci. U. S. A.* 97 (20), 11050–11055.
- Fischl, B., Sereno, M.I., Dale, A.M., 1999. Cortical surface-based analysis. II: inflation, flattening, and a surface-based coordinate system. *NeuroImage* 9 (2), 195–207.
- Fischl, B., van der Kouwe, A., Destrieux, C., Halgren, E., Segonne, F., Salat, D.H., et al., 2004. Automatically parcellating the human cerebral cortex. *Cereb. Cortex* 14 (1), 11–22.
- Fleming, J., Chiang, C., 2015. The Purkinje neuron: a central orchestrator of cerebellar neurogenesis. *Neurogenesis* 2 (1) Austin, Tex. (e1025940).
- Flores, C.E., Mendez, P., 2014. Shaping inhibition: activity dependent structural plasticity of GABAergic synapses. *Front. Cell. Neurosci.* 8, 327.
- Gambardella, A., Marini, C., 2009. Clinical spectrum of *SCN1A* mutations. *Epilepsia* 50 (Suppl. 5), 20–23.
- Guerrini, R., Striano, P., Catarino, C., Sisodiya, S.M., 2011. Neuroimaging and neuropathology of Dravet syndrome. *Epilepsia* 52 (Suppl. 2), 30–34.
- Iskan, Z., Jin, T.B., Kendrick, A., Szeglin, B., Lu, H., Trivedi, M., et al., 2015. Test-retest reliability of freesurfer measurements within and between sites: effects of visual approval process. *Hum. Brain Mapp.* 36 (9), 3472–3485.
- Kalume, F., Yu, F.H., Westenbroek, R.E., Scheuer, T., Catterall, W.A., 2007. Reduced sodium current in Purkinje neurons from Nav1.1 mutant mice: implications for ataxia in severe myoclonic epilepsy in infancy. *J. Neurosci.* 27 (41), 11065–11074 *The Official Journal of the Society for Neuroscience*.
- Marini, C., Scheffer, I.E., Nabbout, R., Suls, A., De Jonghe, P., Zara, F., et al., 2011. The genetics of Dravet syndrome. *Epilepsia* 52 (Suppl. 2), 24–29.
- Mesulam, M.M., 1998. From sensation to cognition. *Brain* 121 (Pt 6), 1013–1052.
- Mistry, A.M., Thompson, C.H., Miller, A.R., Vanoye, C.G., George Jr., A.L., Kearney, J.A., 2014. Strain- and age-dependent hippocampal neuron sodium currents correlate with

- epilepsy severity in Dravet syndrome mice. *Neurobiol. Dis.* 65, 1–11.
- Moehring, J., von Spiczak, S., Moeller, F., Helbig, I., Wolff, S., Jansen, O., et al., 2013. Variability of EEG-fMRI findings in patients with SCN1A-positive Dravet syndrome. *Epilepsia* 54 (5), 918–926.
- Nii, Y., Uematsu, S., Lesser, R.P., Gordon, B., 1996. Does the central sulcus divide motor and sensory functions? Cortical mapping of human hand areas as revealed by electrical stimulation through subdural grid electrodes. *Neurology* 46 (2), 360–367.
- Ogiwara, I., Miyamoto, H., Morita, N., Atapour, N., Mazaki, E., Inoue, I., et al., 2007. Nav1.1 localizes to axons of parvalbumin-positive inhibitory interneurons: a circuit basis for epileptic seizures in mice carrying an Scn1a gene mutation. *J. Neurosci.* 27 (22), 5903–5914 The Official Journal of the Society for Neuroscience.
- Perez, A., Garcia-Penton, L., Canales-Rodriguez, E.J., Lerma-Usabiaga, G., Iturria-Medina, Y., Roman, F.J., et al., 2014. Brain morphometry of Dravet syndrome. *Epilepsy Res.* 108 (8), 1326–1334.
- Raichle, M.E., Mintun, M.A., 2006. Brain work and brain imaging. *Annu. Rev. Neurosci.* 29, 449–476.
- Rakic, P., 1988. Specification of cerebral cortical areas. *Science* 241 (4862), 170–176.
- Scheffer, I.E., Berkovic, S.F., 1997. Generalized epilepsy with febrile seizures plus. A genetic disorder with heterogeneous clinical phenotypes. *Brain* 120 (Pt 3), 479–490.
- Scheffer, I.E., Zhang, Y.H., Jansen, F.E., Dibbens, L., 2009. Dravet syndrome or genetic (generalized) epilepsy with febrile seizures plus? *Brain Dev.* 31 (5), 394–400.
- Shaw, P., Kabani, N.J., Lerch, J.P., Eckstrand, K., Lenroot, R., Gogtay, N., et al., 2008. Neurodevelopmental trajectories of the human cerebral cortex. *J. Neurosci.* 28 (14), 3586–3594 The Official Journal of the Society for Neuroscience.
- Striano, P., Mancardi, M.M., Biancheri, R., Madia, F., Gennaro, E., Paravidino, R., et al., 2007. Brain MRI findings in severe myoclonic epilepsy in infancy and genotype-phenotype correlations. *Epilepsia* 48 (6), 1092–1096.
- Tau, G.Z., Peterson, B.S., 2010. Normal development of brain circuits. *Neuropsychopharmacology* 35 (1), 147–168 Official Publication of the American College of Neuropsychopharmacology.
- Tedesco, A.M., Chiricozzi, F.R., Clausi, S., Lupo, M., Molinari, M., Leggio, M.G., 2011. The cerebellar cognitive profile. *Brain* 134 (Pt 12), 3672–3686.
- Tessier, C.R., Broadie, K., 2009. Activity-dependent modulation of neural circuit synaptic connectivity. *Front. Mol. Neurosci.* 2, 8.
- Tsai, M.S., Lee, M.L., Chang, C.Y., Fan, H.H., Yu, I.S., Chen, Y.T., et al., 2015. Functional and structural deficits of the dentate gyrus network coincide with emerging spontaneous seizures in an Scn1a mutant Dravet syndrome model during development. *Neurobiol. Dis.* 77, 35–48.
- Vijayakumar, N., Allen, N.B., Youssef, G., Dennison, M., Yucel, M., Simmons, J.G., et al., 2016. Brain development during adolescence: a mixed-longitudinal investigation of cortical thickness, surface area, and volume. *Hum. Brain Mapp.* 37 (6), 2027–2038.
- Walton, M.E., Behrens, T.E., Buckley, M.J., Rudebeck, P.H., Rushworth, M.F., 2010. Separable learning systems in the macaque brain and the role of orbitofrontal cortex in contingent learning. *Neuron* 65 (6), 927–939.
- Winkler, A.M., Kochunov, P., Blangero, J., Almasy, L., Zilles, K., Fox, P.T., et al., 2010. Cortical thickness or grey matter volume? The importance of selecting the phenotype for imaging genetics studies. *NeuroImage* 53 (3), 1135–1146.
- Wolff, M., Casse-Perrot, C., Dravet, C., 2006. Severe myoclonic epilepsy of infants (Dravet syndrome): natural history and neuropsychological findings. *Epilepsia* 47 (Suppl. 2), 45–48.
- Yu, F.H., Mantegazza, M., Westenbroek, R.E., Robbins, C.A., Kalume, F., Burton, K.A., et al., 2006. Reduced sodium current in GABAergic interneurons in a mouse model of severe myoclonic epilepsy in infancy. *Nat. Neurosci.* 9 (9), 1142–1149.
- Zuberi, S.M., Brunklaus, A., Birch, R., Reavey, E., Duncan, J., Forbes, G.H., 2011. Genotype-phenotype associations in SCN1A-related epilepsies. *Neurology* 76 (7), 594–600.